Stripe disorder and dynamics in the hole-doped antiferromagnetic insulator La5/3Sr1/3CoO4

PHYSICAL REVIEW B **89**, 020405(R) (2014)

Stripe disorder and dynamics in the hole-doped antiferromagnetic insulator $La_{5/3}Sr_{1/3}CoO_4$

T. Lancaster,[1] S. R. Giblin,[2] G. Allodi,[3] S. Bordignon,[3] M. Mazzani,[3] R. De Renzi,[3] P. G. Freeman,[4,5,*] P. J. Baker,[6] F. L. Pratt,[6] P. Babkevich,[7,*] S. J. Blundell,[7] A. T. Boothroyd,[7] J. S. Möller,[7] and D. Prabhakaran[7]

[1]*Centre for Materials Physics, Durham University, South Road, Durham DH1 3LE, United Kingdom*

[2]*School of Physics and Astronomy, Cardiff University, Queen's Buildings, The Parade, Cardiff CF24 3AA, United Kingdom*

[3]*Dipartimento di Fisica e Scienze della Terra, Università degli Studi di Parma, Viale G. Usberti 7A, I-43100 Parma, Italy*

[4]*Helmholtz-Zentrum Berlin für Materialien und Energie, Hahn-Meitner-Platz 1, DE-14109 Berlin, Germany*

[5]*Institut Laue-Langevin, BP 156, F-38042 Grenoble Cedex 9, France*

[6]*ISIS Facility, Rutherford Appleton Laboratory, Chilton, Oxfordshire OX11 0QX, United Kingdom*

[7]*Department of Physics, Clarendon Laboratory, Oxford University, Parks Road, Oxford OX1 3PU, United Kingdom*

(Received 5 November 2013; published 15 January 2014)

We investigate the magnetic ordering and dynamics of the stripe phase of $La_{5/3}Sr_{1/3}CoO_4$, a material shown to have an hourglass magnetic excitation spectrum. A combination of muon-spin relaxation, nuclear magnetic resonance, and magnetic susceptibility measurements strongly suggest that the physics is determined by a partially disordered configuration of charge and spin stripes whose frustrated magnetic degrees of freedom are dynamic at high temperature and which undergo an ordering transition around 35 K with coexisting dynamics that freeze out in a glassy manner as the temperature is further reduced.

DOI: 10.1103/PhysRevB.89.020405 PACS number(s): 75.47.Lx, 75.50.Lk, 76.75.+i

The hourglass spectrum of spin excitations observed using inelastic neutron scattering (INS) in the cuprate superconductors [1–13] has been linked to the occurrence of alternating patterns of spin and charge stripes in the copper oxide planes [14]. Although many cuprates exhibit hourglass dispersion and show no evidence for stripe order, the discovery of such an excitation spectrum in stripe-ordered cobaltate materials provided strong evidence that the hourglass dispersion results from short-range stripe correlations [15,16]. The main features of the hourglass spectrum can be reproduced by the spin-wave spectrum of perfectly ordered, weakly coupled antiferromagnetic (AFM) stripes [Fig. 1(a)] with phenomenological broadening [15]. Recently, however, a more detailed agreement has been obtained by a spin-wave calculation based on a stripe model that explicitly incorporates quenched disorder in the charge degrees of freedom and whose magnetic moments, through frustration, may be described in terms of cluster-glass behavior at low temperature [17]. (We also note here the more recent observation of an hourglass spectrum in another cobaltate material, within the checkerboard charge-ordered regime, where stripes have not been observed and where an alternative origin for the spectrum is suggested [18].)

The wider implications of the link between stripes and hourglass dispersion, on the cuprates in particular, has motivated this investigation into an aspect of the stripe phase dynamics in $La_{5/3}Sr_{1/3}CoO_4$. The study of very-low-frequency excitations related to stripes, such as their slow collective motion, is outside the scope of inelastic neutron scattering. We have therefore selected muon-spin relaxation (μ^+SR) and nuclear magnetic resonance (NMR) as probes of this behavior. We note that, in contrast to muon and NMR spectroscopy, the previous INS measurements were insensitive to fluctuations on time scales much slower than $\hbar/\Delta E \approx 10^{-11}$ s (where $\Delta E \approx 1$ meV is the energy scale of the resolution of the measurement) and so fluctuations on time scales longer than this appeared static. INS therefore took a "snapshot" of the behavior compared to μ^+SR and NMR measurements whose characteristic time scale is set by the respective gyromagnetic ratios of the muon ($\gamma_\mu = 2\pi \times 135.5$ MHz T^{-1}) and the nuclei being interrogated. In this Rapid Communication we show that μ^+SR and NMR find dynamics, magnetic ordering (around 35 K), and a freezing of dynamically fluctuating moments (around 20 K) which is consistent with a picture of partially disordered stripes whose dynamics are frozen out as the temperature is lowered.

The $La_{2-x}Sr_xCoO_4$ system is based around well isolated, square layers of CoO_2 and is isostructural to the "214" family of cuprates, which includes $La_{2-x}Sr_xCuO_4$. In the parent ($x = 0$) compound, commensurate AFM order has been reported below [19] $T = 275$ K. Hole doping of the material involves exchanging Sr for La, resulting in the donation of positive charges to the CoO layers. For a doping of $x > 0.3$, magnetic order is modulated at 45° to the CoO bonds, which is attributable to the self-organization of holes into arrays of charged stripes, which creates antiphase domain walls in the antiferromagnetic order [20]. The stripe order in $La_{5/3}Sr_{1/3}CoO_4$ involves diagonal lines of nonmagnetic $S = 0$ Co^{3+} ions separated by bands of antiferromagnetically aligned Co^{2+} $S = 3/2$ ions, with intra- (J) and interstripe (J') antiferromagnetic exchange couplings as shown in Fig. 1(a). It is currently assumed that the charge ordering of the Co ions sets in at a temperature T_{CO} well above room temperature, while magnetic Bragg peaks are observed in neutron diffraction below [21] ∼100 K. The correlation lengths of the magnetic order were estimated to be $\xi = 10$ Å parallel to the stripes, and $\xi = 6.5$ Å perpendicular to them, indicating that the magnetism has a short-ranged character, which is unlikely to show conventional critical dynamics [15]. Disordered stripes may be formed by rearranging the charges of the configuration shown in Fig. 1(a). Imperfections in the charge order are expected to be static at temperatures which are low compared to T_{CO} owing to the insulating nature of the material, while dynamic fluctuations should be expected

*Current address: Laboratory for Quantum Magnetism, Ecole Polytechnique Fédérale de Lausanne, CH-1015 Lausanne, Switzerland.

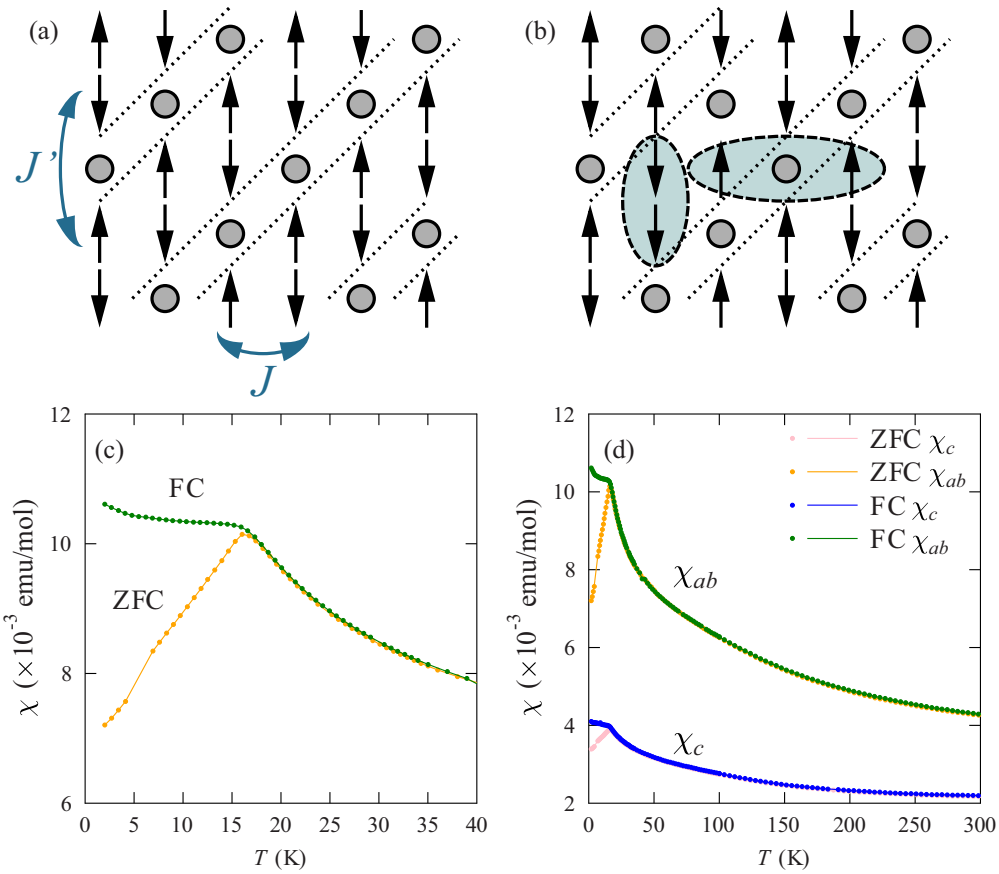

FIG. 1. (Color online) (a) Perfect stripe order in the CoO_2 planes. (Circles represent nonmagnetic Co^{3+}, and arrows represent $S = 3/2$ Co^{2+} spins.) (b) Disordering the charges leads to unfavorable exchange interactions between spins (shaded). (c) and (d) Magnetic susceptibility as a function of temperature for field-cooled and zero-field-cooled protocols for two crystal orientations.

in the spin degrees of freedom below room temperature. As shown in Fig. 1(b), the introduction of charge disorder frustrates the antiferromagnetic coupling between spins, and this is the origin of the proposed cluster-glass behavior in this system [17].

To investigate spin ordering and dynamics, μ^+SR measurements [22,23] were made with the initial muon spin directed along the c axis of the material, so that the muon spins are initially perpendicular to the CoO_2 layers. To survey the slow dynamics of the system, μ^+SR data were measured using the EMU instrument at the ISIS facility [Fig. 2(a)], where time resolution limitations do not allow us to resolve oscillations or relaxation rates $\gtrsim$10 MHz. Instead, we see a decrease in the relaxing amplitude $A_{\rm rel}$ as the material is cooled below 40 K [inset, Fig. 2(b)]. This is because the local field in the ordered state strongly depolarizes the muon spin if local field components are perpendicular to the initial muon-spin polarization, removing relaxing asymmetry from the spectrum. In view of the limitations caused by the ISIS time resolution, we parametrize the muon asymmetry with a stretched exponential function $a(t) = a(0)P(t) = A_{\rm rel}e^{-(\lambda t)^\beta} + a_{\rm bg}$, where $P(t)$ is the muon ensemble spin polarization and $a_{\rm bg}$ is a background contribution. We expect that [23], in the fast fluctuation limit, the muon relaxation rate is determined by the relation $\lambda \propto \Delta^2\tau$, where $\Delta^2 = \gamma_\mu^2\langle B_i^2\rangle$ and τ is the correlation time. We note that no features are observed around 100 K, where magnetic Bragg peaks become resolvable. Three regions in temperature are apparent in the behavior. On cooling in the paramagnetic region I ($T > 40$ K), the relaxation rate λ increases slowly, then more rapidly below ≈ 70 K before peaking at $T = 39$ K [Fig. 2(b)]. The initial polarization $P(t = 0)$ falls slowly across region I. On entering region II ($20 \lesssim T \leqslant 39$ K), $P(0)$ drops rapidly and λ decreases, reaching a minimum at 20 K. Finally, in region III ($T \lesssim 20$ K), $P(0)$ increases and there is another peak in λ centered around 15 K.

A more complete picture of the muon response is obtained from measurements made using the DOLLY instrument at the Swiss Muon Source (SμS) where shorter time scales may be resolved [Figs. 2(c)–2(f)]. In region I we observe rapidly and slowly relaxing contributions with relaxation rates $T_{1\rm f}^{-1}$ and $T_{1\rm s}^{-1}$, respectively. In regions II and III ($T \lesssim 39$ K) we observe oscillations in the muon spectra at early times ($t \leqslant 0.05$ μs), characteristic of a static local magnetic field at the muon stopping site, causing a coherent precession of the spins of those muons with a component of their spin polarization perpendicular to this local field. The frequency of the oscillations is given by $\nu_i = \gamma_\mu B_i/2\pi$, where B_i is the average magnitude of the local magnetic field at the ith muon site. In this temperature regime, two relaxing terms account for the longitudinal component of the asymmetry and two oscillatory terms provide the transverse asymmetry component

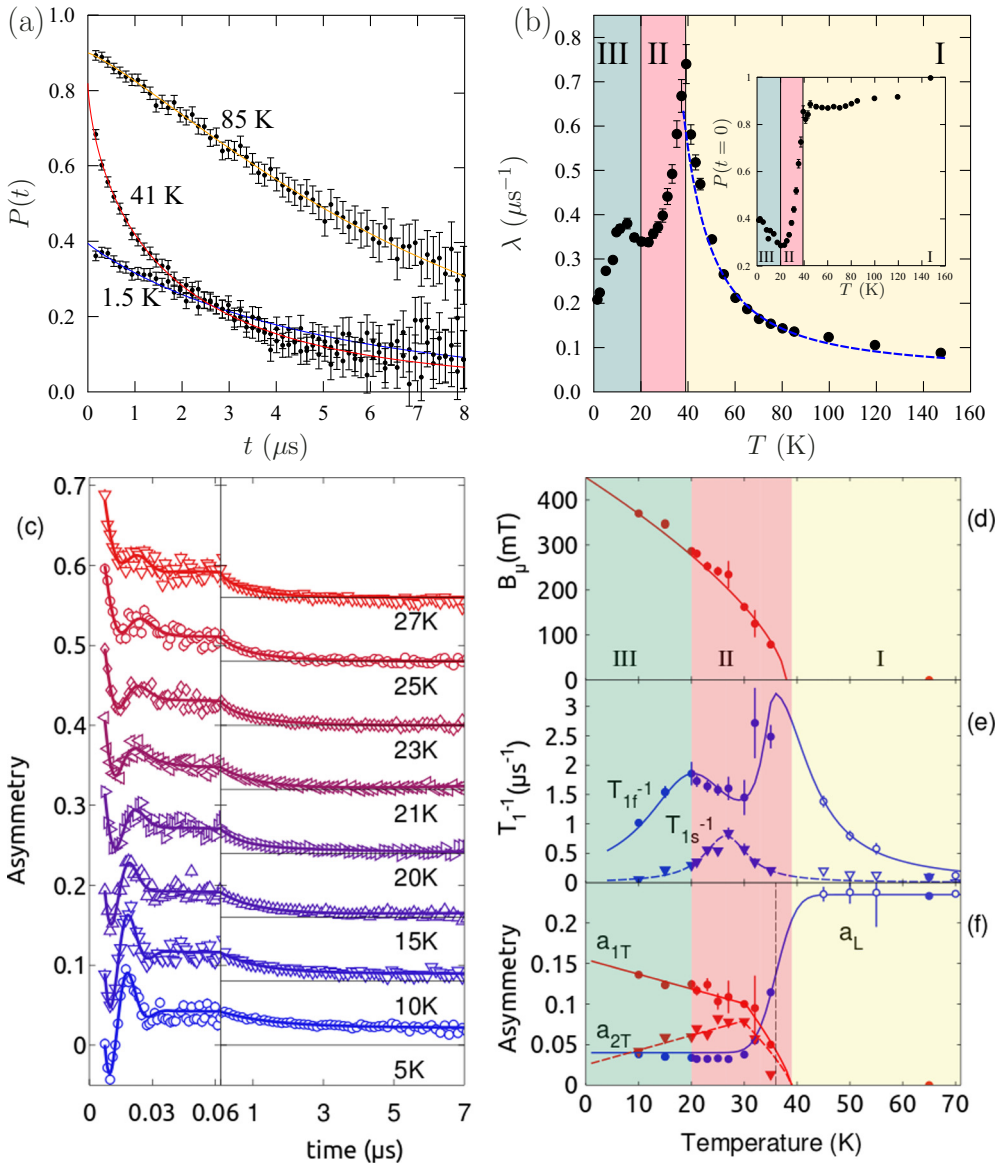

FIG. 2. (Color online) (a) Example zero-field μ^+SR spectra measured at ISIS. (b) ISIS relaxation rate λ with a fit to an activated behavior at high temperatures (see main text). Inset: Initial muon polarization $P(0)$. (c) Data measured at SμS showing oscillations at early times. (d) The larger of the two precession frequencies as a function of temperature. (e) Evolution of longitudinal relaxation rates $1/T_1$. (f) Amplitudes of the transverse and longitudinal components.

[24]. Data in Figs. 2(c) and 2(f) show the presence of these transverse terms in the early-time oscillations and longitudinal terms in the late-time relaxation. The ratio of the two local fields was found to be constant [24] and Fig. 2(d) shows the largest of them as a function of temperature, which is found to vanish at $T_N \approx 35$ K. Figure 2(f) shows that the total amplitude of the transverse terms, $a_{1T} + a_{2T}$, vanishes above T_N, where the total longitudinal amplitude $a_L = a_s + a_f$ recovers the full asymmetry (the distinction between longitudinal and transverse being lost above T_N, where the spin system recovers rotational invariance). On the strength of μ^+SR, we are therefore able to identify a transition to magnetic order around $T_N = 35$ K, broadened by significant inherent static disorder, leading to a Gaussian width $\Delta T_N \approx 5$ K.

The presence of significant static disorder is confirmed by the broad distribution of local fields providing the fast damping of the oscillations [Fig. 2(c)]. The dynamics driving the two longitudinal relaxation rates also deviate from the behavior expected for a homogeneous magnetically ordered phase, for which we expect monotonically increasing relaxation rates up to a critical divergence at T_N [25]. In contrast, Fig. 2(e) suggests not only a peak in T_{1f}^{-1} around T_N significantly broadened in the presence of strong disorder (see, e.g., Ref. [26]), but also shows additional peaks in T_{1f}^{-1} and T_{1s}^{-1} around the crossover between region II and III near 20 K. As argued below, these results are consistent with region II, in addition to showing magnetic order, also displaying significant dynamics which freeze out on cooling, with correlation times starting to become longer than the μ^+SR time window in the more static and ordered region III. This implies that the border between region II and III is actually a blurred crossover.

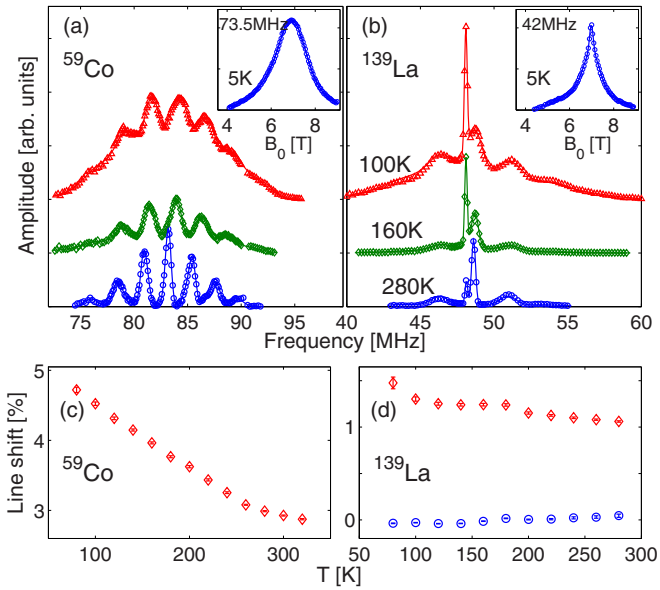

FIG. 3. (Color online) Top: Frequency-swept (a) ^{59}Co and (b) ^{139}La NMR spectra in $B_{app} = 8$ T at three selected temperatures. Insets: Field-swept spectra at 5 K. Bottom: Shifts of (c) the central line of ^{59}Co, and (d) the central doublet of ^{139}La as a function of temperature.

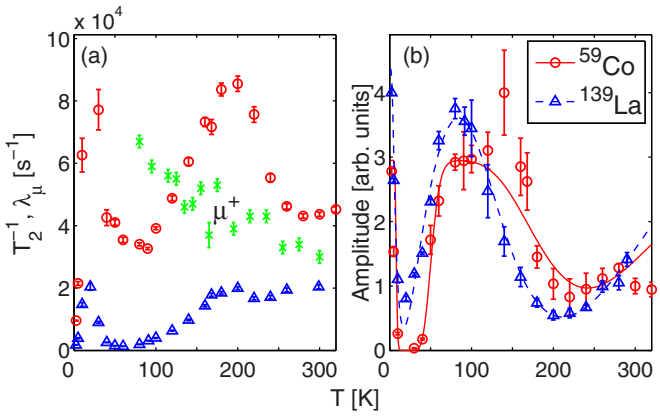

FIG. 4. (Color online) (a) Evolution of spin-spin relaxation rates T_2^{-1} with T for ^{59}Co (circles), ^{139}La (triangles), and muon relaxation rates λ (crosses). (b) Integrated spectral amplitudes, corrected for T_2^{-1} relaxation, as a function of temperature.

To probe the slow dynamics of both charge and magnetic degrees of freedom, NMR measurements were made on a single crystal sample of $La_{5/3}Sr_{1/3}CoO_4$ with an external field applied in the ab plane. We expect that only ^{59}Co nuclei in spinless Co^{3+} ions will be detected, since, for a magnetic Co^{2+} ion, the ^{59}Co nucleus experiences an instantaneous hyperfine field of order 10 Tμ_B^{-1}, whose fluctuations lead to very fast nuclear relaxation [27].

Example frequency-swept spectra from probe nuclei ^{59}Co and ^{139}La, measured in $B_{app} = 8$ T, are shown in Figs. 3(a) and 3(b) (field-swept data shown inset). At room temperature, the ^{59}Co spectrum consists of a well-resolved line septet, originating from the nuclear $I = 7/2$ spin, split by the quadrupole coupling with the local electric field gradient (EFG). The central line, unperturbed to first order by the EFG, exhibits a sizable shift with respect to the ^{59}Co reference [Fig. 3(c)]. The hyperfine coupling of ^{59}Co is estimated as ≈ 5 T from the comparison of the shift with the magnetic susceptibility (see below), a value compatible with a transferred hyperfine contribution from neighboring Co^{2+} onto the nonmagnetic Co^{3+}, confirming the localization of holes in the layers. The ^{139}La ($I = 7/2$) signal shows similar quadrupolar patterns, with higher-order satellites smeared out by EFG inhomogeneities which are larger at the La site. The central line is split into a doublet by magnetic interactions resulting from the occupancy of the nearest neighbor Co site by high-spin Co^{2+} or spinless Co^{3+}. The majority ^{139}La peak exhibits larger and temperature-dependent shifts, while the smaller shift of the minority peak is nearly temperature independent [Fig. 3(d)].

On cooling, the spectra broaden, most dramatically seen in the ^{59}Co signal, which shows a broad shoulder superimposed on the quadrupole septet at 100 K [Fig. 3(a)]. Such broadening reflects the onset of significant magnetic correlations below approximately the same temperature as the onset of magnetic Bragg peaks in neutron scattering [21]. It is likely that the static order here is short ranged and results from the large applied field B_{app}. Line broadening continues on cooling without abrupt changes, with almost featureless spectra observed for $T < 10$ K [Fig. 3 (insets)].

The key result from our NMR is that the signal amplitude is partially lost (or wiped out) in two temperature intervals: above 100 K and, more severely, in the 10–40 K range. We note that the measured spin-spin relaxation rates T_2^{-1} [Fig. 4(a)] exhibit two maxima: a broad peak around 200 K, and a sharper one at $T \approx 20$ K. Where the relaxation rates of the two nuclei develop peaks [Fig. 4(a)], the corresponding amplitudes, corrected for the initial deadtime and the Curie temperature dependence, are severely reduced [Fig. 4(b)], implying that they correspond to residual signals. Faster spin-spin relaxations manifest themselves as sizable missing fractions (i.e., a signal wipeout), coinciding with the T_2^{-1} peaks. A wipeout reflects a broad distribution of relaxation rates, where signal components with T_2 much shorter than the instrumental dead time (≈ 10 μs) are lost. A model of the NMR wipeouts which assumes a log-normal distribution of activation energies [24] suggests a characteristic energy scale for the two distinct observed T_2^{-1} peaks at $E_a \approx 1100$ and 70 K.

Both peaks are indicative of very slow dynamic excitations of the stripes. These slow excitations may involve either separate charge and spin degrees of freedom or their interplay. We are able to discriminate this aspect by comparing the relaxation of the two nuclei with that of the muons. Both nuclei are sensitive to slow dynamics of spin and charge as well, since they are coupled to the EFG via their quadrupole moment. The fast relaxations of ^{59}Co and ^{139}La above 100 K have no counterpart in our μ^+SR data [Figs. 4(a)], and therefore must be due to EFG fluctuations, to which $I = 1/2$ muons are not sensitive. The excitations underlying such EFG fluctuations most likely consist of thermally assisted hopping of holes across stripes, apparently taking place well below the charge-ordering temperature. Such charge motion slows down on cooling, down to a complete freezing at temperatures of the order of 100 K, at which the full NMR signal amplitude

is recovered. The origin of the low-temperature wipeout is magnetic, as described below.

Measurements of dc magnetic susceptibility χ, made using a Quantum Design magnetic property measurement system (MPMS) [Figs. 1(c) and 1(d)], show no strong features around 100 K [Fig. 1(d)] where magnetic Bragg peaks start to appear in neutron diffraction. Susceptibilities measured after zero-field-cooling (ZFC) and field-cooling (FC) protocols (measuring field of $B = 100$ mT) show a gradual increase upon cooling before splitting below $T = 18$ K [Fig. 1(c)]. This splitting is typical of a freezing of the magnetic moments at low temperature and reflects the fact that, after cooling in zero field (ZF) to a region where the spins are statically frozen, we obtain a configuration which is less susceptible to magnetization than occurs if the frozen state is achieved in an applied field. ac susceptibility measurements were attempted on this system but a response could not be resolved.

Taken together, the μ^+SR, NMR, and magnetic susceptibility results allow an insight into the behavior of the stripe ordering and dynamics in $La_{5/3}Sr_{1/3}CoO_4$. *Region I*: The snapshot taken by neutron diffraction indicates that ordered stripes have formed and are static over intervals $\tau > 10^{-11}$ s, at temperatures below 100 K. However, the μ^+SR suggests that, at these high temperatures, spins within the stripes are rapidly fluctuating on the muon (μs) time scale. A crude estimate suggests that the observed muon relaxation rate, of order 0.15 μs^{-1}, is consistent with a local magnetic field of around 150 mT fluctuating with correlation times of order 10^{-11} s. A decrease in temperature causes these fluctuations to slow down, increasing τ and hence λ. Assuming an activated behavior of the fluctuations in this region [Fig. 2(b)] with $\tau = \tau_\infty e^{E_a/T}$, we obtain an activation energy $E_a \approx 100$ K, in reasonable agreement with the energy scale identified from NMR. *Region II*: Temperature $T \approx 40$ K marks the point where stripe spins lock together on the muon time scale and we enter a regime of magnetic order. As the system is cooled through the 40–20 K region, slow dynamics remain significant, leading to the low-temperature NMR wipeout as well as to the muon T_{1f}^{-1} peak. Assuming a simple Lorentzian spectral density, the maximum T^{-1} relaxation rate seen in the μ^+SR data around 20 K [Fig. 2(e)] occurs [24] when $\tau^{-1}(T) = \gamma_\mu B$, where B is the internal magnetic field. Taking $B = 300$ mT when $T_1^{-1} = 2 \times 10^6$ s^{-1} implies $\tau(T \approx 20\ \text{K}) \approx 4$ ns and $\Delta \approx 30\ \mu s^{-1}$. For comparison, the log-normal distribution of correlation times obtained from the ^{59}Co wipeout in NMR [Fig. 4 (Ref. [24]] predicts a range of correlation times $5 \times 10^{-10} < \tau < 8 \times 10^{-9}$ s for $T = 20$ K, in good agreement. *Region III*: Peaks in the muon λ and T^{-1} and the increase in A_{rel} below 20 K suggest a crossover to a more static configuration pointing to the dynamics of the stripes freezing out below 20 K. This low-temperature freezing accounts for the splitting of the ZFC and FC χ data and the reappearance of the NMR signal.

We may compare our results to others measured on stripe-ordered nickelate and cuprate systems [28]. Muon measurements on both $La_{5/3}Sr_{1/3}NiO_4$ and the $La_{1.8-x}Eu_{0.2}Sr_xCuO_4$ system show well-resolved oscillations setting in below ordering temperatures $T_N \approx 200$ K, with signatures of stripe dynamics seen in anomalies in the precession frequencies and/or the longitudinal relaxation rate [28]. In $La_{5/3}Sr_{1/3}NiO_4$, where NMR measurements are suggestive of glassy stripe dynamics [29], the muon and NMR T_1^{-1} both decrease monotonically with decreasing temperature for $T < 200$ K, in contrast to what we report here. However, the correlation length in the nickelate system, estimated [30] as $\xi \gtrsim 100$ Å, is far larger than that of $La_{5/3}Sr_{1/3}CoO_4$, making it hard to see how similar quenched charge disorder drives the physics in that case. For the Eu-containing cuprate system, where NMR shows a low-temperature wipeout and there is evidence for a distribution of time scales [31], it is possible that the broad peak [28] around 7 K measured in the μ^+SR $1/T_1$ has a similar origin to the behavior we observe.

In conclusion, the stripes that dominate the low-energy physics of $La_{5/3}Sr_{1/3}CoO_4$ order on the muon time scale around 35 K, but display slow dynamics that freeze out of spin dynamics upon cooling below 20 K. The distribution of activated spin correlation times detected by both muons and NMR indicate glassy behavior which is most probably due to the inherent frustration introduced by charge disorder in the magnetic couplings. However, the presence of a high-temperature wipeout in the NMR, which has no analog in μ^+SR, indicates that this charge quenching is not complete. The influence of such stripe phase dynamics on the physics of the cuprates remains an open and intriguing question [17].

Part of this work was carried out at the SμS, Paul Scherrer Institut, Switzerland and at the STFC ISIS facility, U.K., and we are grateful for the provision of beamtime. We thank R. Scheuermann and A. Amato for technical support. We thank EPSRC (U.K.) for financial support.

[1] M. Arai, T. Nishijima, Y. Endoh, T. Egami, S. Tajima, K. Tomimoto, Y. Shiohara, M. Takahashi, A. Garrett, and S. M. Bennington, Phys. Rev. Lett. **83**, 608 (1999).

[2] P. Bourges, Y. Sidis, H. F. Fong, L. P. Regnault, J. Bossy, A. Ivanov, and B. Keimer, Science **288**, 1234 (2000).

[3] S. M. Hayden, H. A. Mook, P. Dai, T. G. Perring, and F. Dogan, Nature (London) **429**, 531 (2004).

[4] D. Reznik, P. Bourges, L. Pintschovius, Y. Endoh, Y. Sidis, T. Masui, and S. Tajima, Phys. Rev. Lett. **93**, 207003 (2004).

[5] C. Stock, W. J. L. Buyers, R. A. Cowley, P. S. Clegg, R. Coldea, C. D. Frost, R. Liang, D. Peets, D. Bonn, W. N. Hardy, and R. J. Birgeneau, Phys. Rev. B **71**, 024522 (2005).

[6] V. Hinkov, P. Bourges, S. Pailhes, Y. Sidis, A. Ivanov, C. D. Frost, T. G. Perring, C. T. Lin, D. P. Chen, and B. Keimer, Nat. Phys. **3**, 780 (2007).

[7] B. Fauqué, Y. Sidis, L. Capogna, A. Ivanov, K. Hradil, C. Ulrich, A. I. Rykov, B. Keimer, and P. Bourges, Phys. Rev. B **76**, 214512 (2007).

[8] G. Xu, G. D. Gu, M. Hücker, B. Fauqué, T. G. Perring, L. P. Regnault and J. M. Tranquada, Nat. Phys. **5**, 642 (2009).
[9] N. B. Christensen, D. F. McMorrow, H. M. Rønnow, B. Lake, S. M. Hayden, G. Aeppli, T. G. Perring, M. Mangkorntong, M. Nohara, and H. Tagaki, Phys. Rev. Lett. **93**, 147002 (2004).
[10] B. Vignolle, S. M. Hayden, D. F. McMorrow, H. M. Rønnow, B. Lake, C. D. Frost, and T. G. Perring, Nat. Phys. **3**, 163 (2007).
[11] M. Matsuda, M. Fujita, S. Wakimoto, J. A. Fernandez-Baca, J. M. Tranquada, and K. Yamada, Phys. Rev. Lett. **101**, 197001 (2008).
[12] O. J. Lipscombe, B. Vignolle, T. G. Perring, C. D. Frost, and S. M. Hayden, Phys. Rev. Lett. **102**, 167002 (2009).
[13] J. M. Tranquada, H. Woo, T. G. Perring, H. Goka, G. D. Gu, G. Xu, M. Fujita, and K. Yamada, Nature (London) **429**, 534 (2004).
[14] J. M. Tranquada, Physica B **407**, 1771 (2012), and references therein.
[15] A. T. Boothroyd, P. Babkevich, D. Prabhakaran, and P. G. Freeman, Nature (London) **471**, 341 (2011).
[16] S. M. Gaw, E. C. Andrade, M. Vojta, C. D. Frost, D. T. Adroja, D. Prabhakaran, and A. T. Boothroyd, Phys. Rev. B **88**, 165121 (2013).
[17] E. C. Andrade and M. Vojta, Phys. Rev. Lett. **109**, 147201 (2012).
[18] Y. Drees, D. Lamago, A. Piovano, and A. C. Komarek, Nat. Commun. **4**, 2449 (2013).
[19] K. Yamada, M. Matsuda, Y. Endoh, B. Keimer, R. J. Birgeneau, S. Onodera, J. Mizusaki, T. Matsuura, and G. Shirane, Phys. Rev. B **39**, 2336 (1989).
[20] M. Cwik, M. Benomar, T. Finger, Y. Sidis, D. Senff, M. Reuther, T. Lorenz, and M. Braden, Phys. Rev. Lett. **102**, 057201 (2009).
[21] See Supplementary information in Ref. [15].
[22] S. J. Blundell, Contemp. Phys. **40**, 175 (1999).
[23] A. Yaouanc and P. Dalmas de Réotier, *Muon Spin Rotation, Relaxation and Resonance* (Oxford University Press, Oxford, U.K., 2010).
[24] See Supplemental Material at http://link.aps.org/supplemental/10.1103/PhysRevB.89.020405 for a detailed description of the data fitting.
[25] R. De Renzi, G. Guidi, P. Podini, R. Tedeschi, C. Bucci, and S. F. J. Cox, Phys. Rev. B **30**, 197 (1984).
[26] F. Coneri, S. Sanna, K. Zheng, J. Lord, and R. De Renzi, Phys. Rev. B **81**, 104507 (2010).
[27] A. J. Freeman and R. E. Watson, in *Magnetism IIA*, edited G. T. Rado and H. Suhl (Academic, New York, 1965).
[28] H.-H. Klauss, J. Phys.: Condens. Matter **16**, S4457 (2004); Physica C **481**, 101 (2012).
[29] Y. Yoshinari, P. C. Hammel, and S.-W. Cheong, Phys. Rev. Lett. **82**, 3536 (1999).
[30] H. Yoshizawa, T. Kakeshita, R. Kajimoto, T. Tanabe, T. Katsufuji, and Y. Tokura, Phys. Rev. B **61**, R854 (2000).
[31] N. J. Curro, P. C. Hammel, B. J. Suh, M. Hücker, B. Büchner, U. Ammerahl, and A. Revcolevschi, Phys. Rev. Lett. **85**, 642 (2000).